

Osteoarthritis and Cartilage



The OARSI histopathology initiative – recommendations for histological assessments of osteoarthritis in the rat

N. Gerwin †^{*,a}, A.M. Bendele ‡^a, S. Glasson §, C.S. Carlson ||

† Novartis Institutes for BioMedical Research, Musculoskeletal Disease Area, 4002 Basel, Switzerland

‡ BolderBioPATH Inc., University of Colorado, MCD Biology, Boulder, CO, USA

§ Pfizer, Cambridge, MA, USA

|| College of Veterinary Medicine, University of Minnesota, St. Paul, MN, USA

ARTICLE INFO

Article history:

Received 1 May 2010

Accepted 5 May 2010

Keywords:

Score
Cartilage
Degeneration
Chondrocyte
Sectioning
Staining

SUMMARY

Objective: During the development of disease-modifying osteoarthritis (OA) drugs, rat models of OA are frequently used for a first assessment of *in vivo* efficacy. The most efficacious compound in the rat model may then be tested in a larger animal model before entering human trials. The aim of this study was to describe a histologic scoring system for use in different models of OA in rats that allows standardization and comparison of results obtained by different investigators.

Methods: The experience of the authors with current scoring systems and the range of lesions observed in rat and human OA studies were considered in recommending this common paradigm for rat histologic scoring. Considerations were made for reproducibility and ease of use for new scorers. Additional scoring paradigms may be employed to further identify specific effects of some disease-modifying drugs.

Results: Although the described scoring system is more complex than the modified Mankin scores, which are recommended for some other species, the reliability study showed that it is easily understood and can be reproducibly used, even by inexperienced scorers.

Conclusions: The scoring paradigm described here has been found to be sufficiently sensitive to discriminate between treatments and to have high reproducibility. Therefore we recommend its use for evaluation of different rat OA models as well as assessment of disease-modifying effects of treatments in these models.

© 2010 Osteoarthritis Research Society International. Published by Elsevier Ltd. All rights reserved.

Introduction

Spontaneous osteoarthritis (OA) is extremely uncommon in rats of all strains, although minor foci of articular cartilage degeneration have been observed^{1,2}. The most commonly used rat OA model is the surgically-induced medial meniscal tear (MMT) model^{3–5}, followed by anterior cruciate ligament transection (ACLT) alone^{6–8} or in combination with (partial) medial meniscectomy (ACLT + pMMx)^{9,10} (Gerwin and Gliem, unpublished data). Few publications describe partial meniscectomy alone^{8,11}. The combination of a surgical model with forced mobilization or high

impact exercise of rats is used to increase severity and/or frequency of OA^{6,10,11}, while moderate-impact exercise appears to decrease OA severity¹². Intra-articular iodoacetate injection^{13–16} is also frequently performed, but it is considered to be a model of cartilage damage, aggressive subchondral bone lesions, inflammation and joint pain caused by chemically-induced chondrocyte death, rather than a model of OA. Models of surgically-created partial and full-thickness cartilage defects in rats are used mainly for gene therapy, stem cell transplantation, artificial cartilage implantation and local growth factor treatment studies^{17–20}. Ovariectomy in rats has been done to model postmenopausal OA in humans²¹, but the observed cartilage lesions are extremely mild and do not progress sufficiently to allow for disease modification studies (S. Glasson, unpublished observations). Transgenic rat models of OA are not yet available, but OA-like pathology was described for mutant strains of rats e.g., homozygous dwarf dw/dw rats, which have reduced growth hormone (GH) levels²². The available rat models are listed in Table I.

* Address correspondence and reprint requests to: Nicole Gerwin, Novartis Institutes for BioMedical Research, Musculoskeletal Disease Area, WKL-125.10.59, 4002 Basel, Switzerland. Tel: 41-61-6962652; Fax: 41-61-6964509.

E-mail address: nicole.gerwin@novartis.com (N. Gerwin).

^a Both authors contributed equally.

Table 1
Models of OA in the rat

Model	Publications	Comments
Spontaneous OA models	<ul style="list-style-type: none"> • Gyarmati <i>et al.</i>¹ • Smale <i>et al.</i>² 	No model exists as spontaneous OA has not been reported to occur in rats. Minor medial degenerative changes may occur.
Induced OA models		
Surgically-induced OA		
MMT	<ul style="list-style-type: none"> • Bendele³ • Janusz <i>et al.</i>⁴ • Moore <i>et al.</i>⁵ • Fernihough <i>et al.</i>²⁴ • Wancket <i>et al.</i>³² • Bove <i>et al.</i>²⁵ • Flannery <i>et al.</i>²⁹ • Baragi <i>et al.</i>²³ • Glasson <i>et al.</i>³³ 	DMOAD activity shown for <ul style="list-style-type: none"> • broad-spectrum MMP inhibitors⁴, • selective MMP-13 inhibitors²³, • selective ADAMTS inhibitors³³, • FGF-18, which indicates that cartilage repair strategies can be evaluated in this model⁵.
ACL T	<ul style="list-style-type: none"> • Williams <i>et al.</i>⁶ • Stoop <i>et al.</i>⁷ • Karahan <i>et al.</i>⁸ • Galois <i>et al.</i>¹² • Hayami <i>et al.</i>²⁶ • Jean <i>et al.</i>³⁴ 	DMOAD activity shown for <ul style="list-style-type: none"> • bisphosphonate Alendronate; protects cartilage and bone²⁶, • COX-2 inhibitor parecoxib; inhibits cartilage degeneration³⁴.
ACL T + pMMx	<ul style="list-style-type: none"> • Hayami <i>et al.</i>⁹ • Appleton <i>et al.</i>¹⁰ • Yorimitsu <i>et al.</i>³⁰ • Gerwin and Gliem, unpublished results 	
pMMx	<ul style="list-style-type: none"> • Karahan <i>et al.</i>⁸ • Lozoya and Flores¹¹ 	
Ovariectomy		
Ovariectomy as a model of postmenopausal OA	<ul style="list-style-type: none"> • Hoeg-Andersen <i>et al.</i>²¹ 	Cartilage lesions are extremely mild and do not progress sufficiently to allow for disease modification studies.
Enzymatic/chemically-induced OA		
Intra-articular iodoacetate injection	<ul style="list-style-type: none"> • Kalbhen¹³ • Guingamp <i>et al.</i>¹⁴ • Guzman <i>et al.</i>¹⁵ • Janusz <i>et al.</i>¹⁶ 	Frequently used as model of joint pain. Morphologic changes in cartilage do not resemble OA lesions. Aggressive subchondral bone lesions form the basis for macroscopic evaluation.
Intra-articular papain injection	<ul style="list-style-type: none"> • Lin <i>et al.</i>³⁵ 	
Intra-articular collagenase injection	<ul style="list-style-type: none"> • Yeh <i>et al.</i>³⁶ 	
Denervation model		
Intra-articular injection of immunotoxin	<ul style="list-style-type: none"> • Salo <i>et al.</i>³⁷ 	
Impact models	None in routine use	
Genetic models		
Transgenic or knockout models	None available	
Mutant strains dw/dw rats	<ul style="list-style-type: none"> • Ekenstedt <i>et al.</i>²² 	Very reproducible, but mild, OA-like lesions.

Commonly used rat surgical OA models

Rat MMT model of OA

Unilateral MMT in mature rats results in rapidly progressive cartilage degenerative changes characterized by chondrocyte and proteoglycan (PG) loss, fibrillation, osteophyte formation, and chondrocyte cloning^{3,4}. Cartilage degenerative changes develop progressively and, by 3–6 weeks post-surgery, may be focally severe on the outer 1/3 of the medial tibia (adjacent to the synovium) with lesions of lesser severity in the middle and inner 1/3 (Fig. 1). Osteophytes progressively increase in size. The model results in total cartilage loss (to eburnated bone) in 12 months in the medial tibia of virtually all rats. Zonal analysis can detect the effects of different types of treatment because the pathogenesis of lesions differs in the three zones of the medial tibia: the outer zone (zone 1-adjacent to the synovium at the medial edge of joint) is subjected to more mechanical forces, while the inner zones (zone 2-central, zone 3-adjacent to the central cruciate ligaments) incur less mechanical forces. Femoral lesions may be highly variable as a result of iatrogenic injury to the femur during surgery.

The MMT model offers the opportunity to evaluate not only chondroprotective effects of agents^{4,23} and cartilage repair strategies⁵, but also bone preserving activities since this model exhibits early subchondral resorptive and later sclerotic bone changes. Effects of treatments on repair of the medial capsule and transected meniscal collateral ligament (MCL) as well as effects on synovium can be studied if joints are left intact for microscopic evaluation. Thickening of the medial joint capsule was, for example, observed after treatment with broad-spectrum matrix metalloproteinase (MMP) inhibitors at 3–13 weeks following MMT induction (S. Glasson *et al.*, unpublished results), probably due to inhibition of matrix degradation during the repair process. Identification of such an increase in capsule thickness is important because capsular fibroplasia may contribute to joint stabilization, serving as an additional mechanism to influence cartilage degradation. More recently, MMT was identified as a model of joint pain, measured as reduction in paw withdrawal thresholds and reduced weight-bearing of the operated leg²⁴. Responsiveness to a cyclooxygenase (COX)-2 inhibitor and a neuropathic pain medication suggests that MMT can also be used as a model for the development of pharmacologic interventions for symptomatic treatment of OA²⁵.

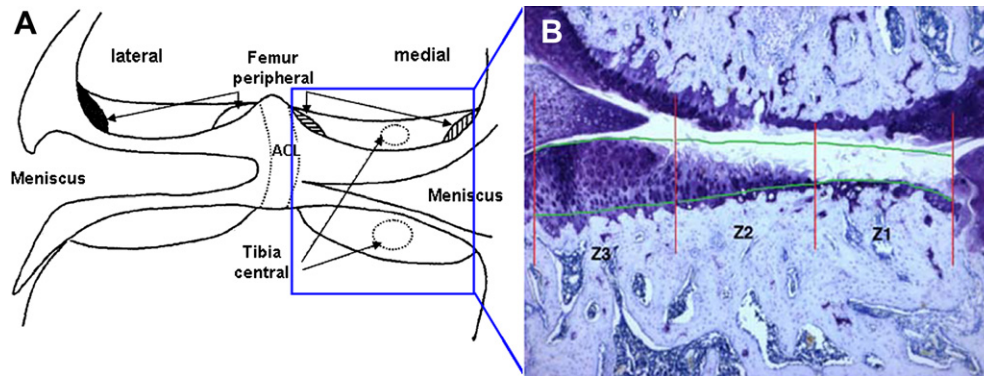


Fig. 1. **A.** Schematic drawing of the rat knee joint after ACLT surgery (image was taken from reference⁷). Areas surrounded by dotted lines are central locations of cartilage degeneration in the medial tibia plateau (MTP) and medial femoral condyle (MFC). Black, open, and striped areas represent peripheral cartilage areas of chondrocyte death in the lateral and medial femur. **B.** Histological section of the MTP and the MFC of a rat with OA lesions 3 weeks after MMT surgery. For evaluation, the tibial plateau is divided into three zones of equal width using an ocular micrometer or a ruler on a photograph, with zone 1 (Z1) on the outside (medial edge of joint) and zone 3 (Z3) on the inside (adjacent to the central cruciate ligaments). Zones are delineated by red lines. The projected cartilage surface and the tidemark are delineated by green tracing.

ACLT combined with ACLT + pMMx and ACLT models of OA

Unilateral surgical ACLT + pMMx in mature rats also leads to the development of progressive cartilage degeneration, but progression is slower than in the MMT model, with focal cartilage erosion developing at 4–12 weeks post-surgery (vs 3–6 weeks in the MMT model)^{9,10} (Gerwin and Gliem, unpublished results). Similar to the MMT model, cartilage lesions develop mainly in the outer 1/3 of the medial tibia, however, in the ACLT + pMMx model, lesions also develop in the medial femur. Osteophytes are detected in 50–75% of the animals, at the outer margins of the medial tibial plateau (MTP), beginning at 4–6 weeks post-surgery (Gerwin and Gliem, unpublished results)⁹. Total cartilage loss can occur, but only at very late time points after surgery (10–12 weeks)^{9,10} (Gliem and Gerwin, unpublished results). Subchondral bone sclerosis is always observed in this model. Progression time of cartilage degeneration is shorter if the MCL is transected⁹ than if it is left intact¹⁰ (Gerwin and Gliem, unpublished results). Furthermore, severity of cartilage degeneration increases proportionally to the amount of the medial meniscus that is removed.

ACLT alone leads to less severe cartilage degeneration and this develops later and progresses more slowly than in the ACLT + pMMx model when the two models are studied side-by-side^{7,9} (Gerwin and Gliem, unpublished results). Focal cartilage fibrillation is observed, but not as reliably as in the ACLT + pMMx model, and no severe cartilage loss is detected after ACLT alone in animals followed up to 12 weeks after surgery. Osteophytes are small or absent. Interestingly, replacement of articular cartilage by fibrocartilage, most frequently detected in the lateral femoral condyle, is a feature of the ACLT model but not the ACLT + pMMx model^{7,9} (Gerwin and Gliem, unpublished results).

To our knowledge, the three models have not been compared side-by-side by a single surgeon using the same histological assessment scheme. However, published data and our own unpublished results suggest that the ACLT + pMMx and the ACLT model, have a slower progression of OA, and result in less severe disease, than the MMT model, particularly if the MCL is not transected. Therefore, the threshold for detecting protective effects of therapeutic interventions is expected to be lower in the ACLT and ACLT + pMMx models than in the MMT model. However, cartilage and bone protective effects in the ACLT model have been published so far for only one therapeutic agent, that being the bone resorption inhibitor Alendronate²⁶.

General considerations for all models

For all rat models of surgically-induced OA it is recommended that skeletally mature animals, 12 weeks of age or older, be used to mimic the development of OA in humans as closely as possible. Young, growing rats develop far less cartilage pathology (S. Glasson, personal communication), presumably because of the higher level of matrix synthesis in younger animals. For many studies, it is optimal to collect serum, urine and synovial fluid for biomarker analysis. A mature growth plate is preferred, since the turnover of this tissue contributes many collagen type II and aggrecan fragments to the serum and urine pool. These considerations could necessitate the use of much older rats, such as the 9-month-old females used by Hoegh-Andersen *et al.*²¹. However, using such aged rats for routine drug discovery studies is not practical and should be reserved for follow-up biomarker studies where the proof-of-concept for disease modification has been clearly established.

Various strains of rats are used, primarily Lewis, Sprague-Dawley (SD) or Wistar rats. While the use of SD rats is often described in the literature, Lewis rats are preferred for the MMT and ACLT + pMMx models. In side-by-side comparisons of Lewis and SD rats in the MMT model, for example, Lewis and SD rats responded differently to the surgery (A. Bendele, unpublished results). Lesions in the Lewis rats are uniformly more severe in the outer 1/3 of the proximal tibia, progressing to less severe lesions in the middle and inner thirds (Fig. 1), whereas the SD rats tend to have lesions of equal or sometimes slightly greater severity in the middle 1/3 than the outer 1/3 and generally develop larger osteophytes than the Lewis rats. SD rats also have a tendency to develop spontaneous cartilage cysts with aging [Fig. 7(A)]. Since it is becoming increasingly popular to carry out OA studies of more than 3 weeks duration, the incidence and severity of these cysts in older SD rats make this a less desirable species than Lewis rats for OA studies.

Variability in the severity of lesions within the same model can occur when the surgery is performed by individuals with non-uniform surgical skills, and this is true of all surgical models. For example, the lesions observed in animals after an individual performs the surgery for the first time are usually quite severe; these tend to decrease in severity as the surgeon gains experience. The reason for this may lie in the extent to which the joint capsule is opened (as this would influence the level of instability in the joint), the period of time the joint is open (potential for drying out), the extent of bleeding (which may cause plasmin activation of MMPs and synovitis), the amount of suture material left in the joint, and

the degree of iatrogenic damage. To minimize the influence of these effects, animals among different treatment groups should be randomized according to surgeon as well as to the order in which they underwent the surgical procedure.

In our opinion, the best model of OA for testing therapeutic interventions is one in which there is a mild-to-moderate rate of progression with a sufficient duration for the development of robust lesions, thus allowing for differentiation among the treatment groups. For example, we have observed in the rat MMT model that while modest treatment efficacy was observed at the 3-week time point, a far more robust response was appreciated at a later time point (3 months), when lesions of cartilage degeneration were more severe (A. Bendele and S. Glasson, unpublished results).

Scoring

Macroscopic staging

Gross evaluation of joints is generally not done for rat surgery models since this would require dissection, which would alter the spatial relationships among the tibia, femur and synovium. Opening the joint also would prevent evaluation of fibrous repair of the joint capsule and changes in the synovium. Nevertheless, macroscopic evaluation of cartilage surfaces is described for the MMT, ACLT + pMMx and ACLT models (Fig. 2).^{4,9,10,26} In unstained tibial plateaus and femoral condyles, surface abrasion and fibrotic tissue are visible as surface roughness and osteophytes are opaque, compared to the smooth, glassy appearance in unoperated joints or sham controls. When the tibial plateaus and femoral condyles are examined grossly after staining with Evan's blue, only the cartilage lesions stain blue and these areas can be quantified by histomorphometry. Greater contrast can be obtained with joints that are stained before fixation compared with those that are fixed before staining. For quantification, the surfaces of tibial plateaus or femoral condyles should be photographed followed by measurement of the total surface area of the joint vs the area of lesion(s) to allow calculation of the % surface area affected.

Microscopic scoring

Recommended methods for processing of joints: fixation, decalcification, embedding, sectioning and staining

Rat joints are most frequently fixed in 10% formaldehyde for about 3 days. Various protocols have been described for decalcification. In our experience decalcification in Immunocal (Decal Chemical Corporation, Tallman, NY) or 5% formic acid for 11–12 days or in 20% ethylenediaminetetraacetic acid (EDTA) for 14–21

days works well for mature rats. Decalcification times need to be adapted, depending on the age of the animals, with the longer time interval used for older animals.

Frontal sectioning

The most frequently used method of embedding and sectioning for microscopic evaluation is frontal sectioning^{4,9,25,26}. To accomplish this, joints are cut into two approximately equal halves, an anterior and a posterior one, along the medial collateral ligament in the frontal plane. This is aided by removing the patella and immobilizing the joint by holding it along the patellar groove and anterior surface of the knee joint with blunt forceps in one hand and restraining the posterior aspect with the other. This somewhat straightens the joint and allows, after positioning the joint on a cutting board, for aligning the cut through the middle of the arms of the forceps with a razor blade. The two resulting tissue pieces (anterior and posterior half) are then both embedded in a single paraffin block with the cut planes facing down. The resulting histological sections will include both femoral condyles, tibial plateaus and menisci, but will not include the trochlear groove or patella.

Three 4–8 μm sections should be cut from each paraffin block at approximately 200 μm steps to obtain three sections from each half (anterior and posterior) of the knee. If the contralateral knee is used as a control (e.g., as a staining controls for quantification of PG loss) it is sufficient to prepare a single section. If frontal sections are done in a consistent manner, 300–325 g rats will have a consistent width across the MTP of approximately 2000 μm . It is important that this measurement is consistent for subsequent measures of degradation across that surface. Sectioning through the entire knee joint may be required when a model is being newly established, in order to ensure that the exact location and entire extent of the lesions are detected.

Coronal sectioning

For preparation of coronal sections⁷ (Gerwin and Gliem, unpublished results), the intact flexed joint is embedded in paraffin, with the patella facing down. The most reproducible results are achieved if the amount of flexion in every knee joint studied is the same, e.g., 120°, which can be achieved by mounting the trimmed knee joint on a plastic triangle with a 120° angle for fixation. Coronal sectioning of the paraffin-embedded, flexed knee joint is started from the anterior aspect of the leg at the patella and is continued posteriorly through the femoral condyles. The knee joint is carefully oriented using the shapes of the growth plates and menisci as hallmarks to ensure that sections are coronal, i.e., all four condyles are sectioned at the same depth. Preparation of sections at 200 μm steps will yield a total of about 10–15 collection points, depending on the age of the rats. If the model is well established, it may be

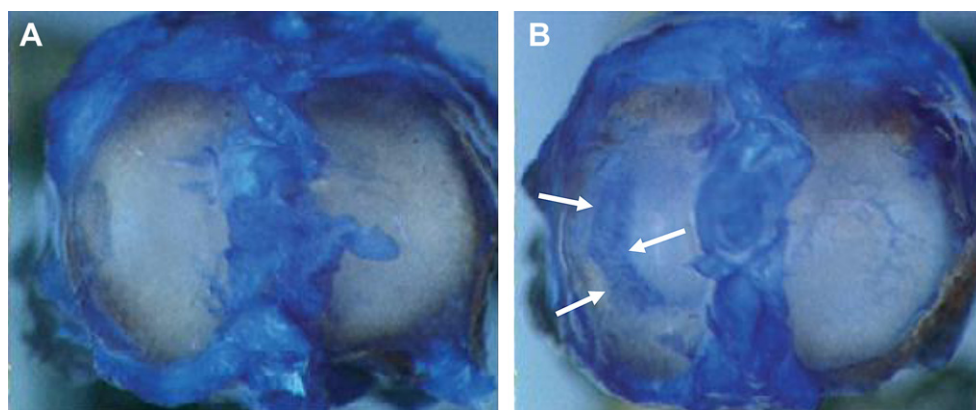


Fig. 2. Macroscopic features of Evan's blue-stained tibial plateaus in the rat MMT model (image was taken from reference⁴). Tibial plateau from **A.** an unoperated rat, and **B.** a rat that had undergone MMT 3 weeks before. Cartilage lesions are apparent on the MTP as crescent-shaped, Evan's blue-stained area (arrows).

sufficient to collect three sections at 200 μm intervals to include areas containing the lesions, similar to the technique for frontal sections. For sectioning through the entire joint, coronal sectioning is more time consuming than the previously-described frontal sectioning method, because only one section is cut at a time. An advantage of this technique, however, is that it offers the opportunity to obtain optimally-oriented midcoronal sections by allowing one to correct the angle of the paraffin block during sectioning.

Sagittal sectioning

The preparation of sagittal sections is described in the literature and involves embedding the joint with the medial (most commonly) or lateral aspect down^{6,8,10}. Sectioning is usually started at the medial margin of the joint. Appleton *et al.*,¹⁰ for example, started collection of sections at about 180 μm from the joint margin and collected about 40 sections at 30 μm intervals across the entire joint.

The choice of sectioning method will be dependent on the location of the lesion in a particular model. Since most instability models have the most severe lesions on the central weight-bearing area of the plateau or condyle, one may assume that measurement of the maximal score or extent of these lesions will yield similar results in sagittal vs frontal or coronal sections. However, to our knowledge, a side-by-side comparison of frontal/coronal and sagittal sections to ensure that this is correct has not been done. A disadvantage of the sagittal sectioning method is that osteophytes, which are frequently found in the medial compartment, are difficult to detect and quantify, since the sections are cut parallel, rather than perpendicular, to the osteophyte. In addition, changes in synovial tissue e.g., synovial inflammation, thickening or pannus formation, are not as easily detectable in sagittal sections as in frontal or coronal sections.

Staining

The most frequently used staining methods are Toluidine blue, Safranin O-Fast Green and Hematoxylin & Eosin (H&E). For the recommended method of scoring (see below) it is important that the stain is sensitive enough to clearly demarcate the tidemark, which is the case for H&E and some methods of Toluidine blue staining (see Supplemental Table I, for staining protocol). Since Toluidine blue and Safranin O stains are relatively specific for cartilage glycosaminoglycans and PGs, these stains can be used to detect areas of PG loss in cartilage. Quantification of cartilage PG staining intensity in Toluidine blue and Safranin O-Fast Green stained sections by histomorphometry is not recommended, even if sections from the contralateral knee are used as staining controls, since binding of both stains appears to be stoichiometric only within a relatively limited range of PG content of the tissue²⁷.

Scoring of sections

Most of the microscopic scoring systems described for rat OA models use modified Mankin scores²⁸, which were originally adapted for other species and include specific adaptations for rats; however, very few of the modifications are described in detail^{4,26,29,30}. Most of these schemes restrict evaluation of OA to cartilage changes, while a few include OA-related changes in bone and synovium. In some of the recently published rat OA studies^{10,30} the OARSI score³¹ is used, which multiplies the cartilage damage score by a factor to reflect the extent of the tibial plateau that is involved.

For a general histological assessment of OA in rats, a modified Mankin score, like the one described for guinea pigs in this issue, may be sufficient. The scoring system that we recommend, however, has proven particularly useful for sensitive detection of the effects of various treatments on the severity of OA. Our recommendation for scoring of frontal sections, prepared as described above, is provided below. Primary and supplemental measures are indicated under each section.

Histologic scoring is performed on the three most severely affected sections. These are selected from either the anterior or posterior sections of the knee from the three slides obtained per knee joint at 200 μm intervals using the frontal sectioning method, or from the three most severely affected consecutive sections (at 200 μm intervals) using the coronal sectioning method. The values for each parameter (listed below) are then averaged across the three scored sections per knee joint.

The scoring methods for the parameters listed below are described for the MTP unless indicated otherwise. The decision whether or not to evaluate the medial and lateral femoral condyles and the lateral tibial plateau, as well, depends on the model. If the model previously has been described and validated and the lesions are most severe in the MTP, it may be sufficient to restrict the scoring to the MTP. If not, the entire joint should be evaluated to determine the location of the most severe lesions.

#1 Cartilage matrix loss width. The progression of cartilage matrix loss in the rat involves superficial fibrillation and loss of matrix initially, followed by a deeper fibrillation/matrix loss through the mid zones and widening of the lesion, eventually resulting in full-thickness loss of matrix to the tidemark in focal or locally extensive regions. In order to assess these progressive changes in an objective manner, the width of the area of collagen matrix loss is measured along the surface (0% depth), as well as at the level of the midzone (50% depth) and tidemark (100% depth; Fig. 3). Only areas of complete cartilage matrix loss are measured; areas of degenerated cartilage affected by only PG or chondrocyte loss are not evaluated. The measurement can be performed by either use of a micrometer directly in the microscope or by capturing an image of the slide and taking measurements using a basic image analysis program. Measures are expressed in microns. Any floating debris in the lesion is ignored.

We recommend to measure in the following order:

- Surface (0% depth): width of any cartilage matrix loss along the projected cartilage surface, where the cartilage on either side has intact superficial cartilage.
- Tidemark (100% depth): width of cartilage matrix loss at the level of the tidemark.
- Midzone (50% depth): width of cartilage matrix loss at the midpoint of the cartilage thickness (between surface and tidemark).

#2 Cartilage degeneration score. This score is an evaluation of overall cartilage pathology and includes the important pathology parameters of collagen matrix fibrillation/loss and chondrocyte death/loss with chondrocyte loss being the primary determinant of the score. PG loss will be present in these areas of matrix and/or chondrocyte loss and, therefore, is also included. Areas of cartilage in which PG loss is present, but which contain no evidence of chondrocyte death, are excluded when evaluating this parameter because these are covered in the total width measure (#3 below). For the cartilage degeneration score, the MTP is divided into three zones in order to evaluate pathology of different load-bearing areas (Fig. 4). Cartilage degeneration in each zone is scored 'none' to 'severe' (numerical values 0–5) using the criteria described in Table II.

A micrometer is placed over the entire width of the load-bearing medial tibial cartilage plateau (from the edge of the osteophyte, or the junction of weight-bearing cartilage with the marginal zone, across the load-bearing surface) to enable dividing the entire width into three regions of equal width, an outer zone 1 (at the medial edge of joint), a central zone 2 and an inner zone 3 (adjacent to the central cruciate ligaments). The original surface of the tissue must be estimated. Then the % area of each zone that contains cartilage

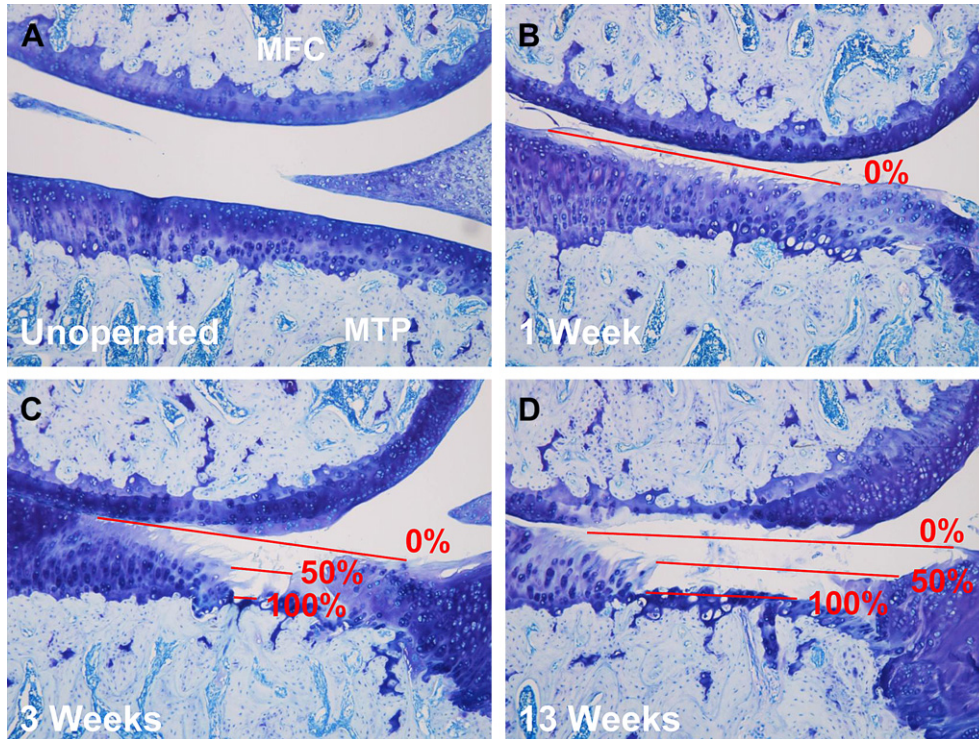


Fig. 3. #1 Cartilage matrix loss width. Histological sections of the MFC and the MTP of unoperated rats (A.) and rats with OA lesions at 1 (B.), 3 (C.) and 13 (D.) weeks following MMT. For evaluation, the widths of collagen matrix loss are measured in relation to the depth of full-thickness non-calcified cartilage matrix. Widths may be measured with a computerized imaging system, a reticule, or on photographs, as long as accurate calibration/micron bar references are utilized. These widths can be tabulated to provide a visual reflection of the lesion architecture and comparisons can be made for these continuous variables in multiple statistical tests. In general, comparisons between the widths at 50% depth of matrix loss across treatment groups and time points are the most sensitive of all of the depth measures at reflecting changes. The width of lesions is measured at 0%, 50% and 100% depths.

exhibiting loss of chondrocytes (50% or greater loss of normal cellularity) or loss of matrix is estimated (or measured with an image analysis program) and a score is assigned to that zone based on that percentage.

A 3-zone-sum for cartilage degeneration is also calculated by adding the values obtained for each zone. The maximum 3-zone-sum for the medial tibia is 15.

The same process is applied to evaluation of the femoral condyles and the lateral tibial plateau, if desired, with the exception that lesions in these sites are not analyzed based on zones since they are not generally distributed over the surface in a zonal pattern. The total width of the load-bearing surface (approximately 2000 μm for femur) should be determined and the same criteria applied as described for evaluating general pathology of tibia to the most severely affected 1/3, 2/3 or 3/3. For example, if 1/3 of the total area (lesion may be in the center of the plateau covering about 667 μm) has minimal degeneration (5–10% of total area has loss of chondrocytes and/or matrix), a grade of 1 is assigned. If that minimal degeneration extends over the entire surface (3/3) then the grade is 3. If the entire femoral cartilage is absent as a result of severe diffuse degeneration, then the grade is 15.

#3 Total cartilage degeneration width. The total width of the area of articular cartilage affected by any type of degenerative change

Table II
#2 Cartilage degeneration score

Parameter	Grade	Description
Cartilage degeneration	0	No degeneration
	1	Minimal degeneration; 5–10% of the total projected cartilage area affected by matrix or chondrocyte loss
	2	Mild degeneration; 11–25% affected
	3	Moderate degeneration; 26–50% affected
	4	Marked degeneration; 51–75% affected
5	Severe degeneration; greater than 75% affected	

(matrix fibrillation/loss, PG loss with or without chondrocyte death) is measured in micrometers. This measurement takes into account foci of minor change (PG loss only), especially in zone 3, that are excluded from the cartilage degeneration score (#2 above). The measurement extends from the point on the cartilage surface where degeneration of the underlying cartilage begins in zone 1, across the area of cartilage degeneration to the point where the tangential layer and underlying cartilage appear histologically normal (Fig. 5). All areas of abnormal matrix across the surface are measured. If there are intervening areas of normal cartilage, they are not included in the measurement. In general, the width of load-bearing cartilage across the tibia is very consistent (2000 μm in a 300 g rat) thus allowing this parameter to be expressed as an absolute value rather than %. However, if sectioning is not consistent and total widths are variable, this parameter needs to be expressed as % of total width.

#4 Significant cartilage degeneration width. This parameter is a measurement of the width of the tibial cartilage in which 50% or greater of the thickness (from surface to tidemark) is seriously compromised (Fig. 5). A cartilage area is considered to be seriously compromised when 50% of chondrocytes are absent or necrotic, with or without collagen matrix loss; therefore, this measurement correlates with the cartilage degeneration score (#2 above). In general, chondrocyte and PG loss are more extensive than the collagen matrix loss and often extend to at least 50% or greater of the cartilage depth in zones 1 and 2. Significant cartilage degeneration width is measured and may be expressed as an absolute value or as percent of total tibial cartilage width. Measurement of this parameter is an easy, rapid method for identifying effects of treatments on more severe cartilage changes, as it only includes moderate to severe degeneration and excludes minimal to mild changes (covered in other measures).

#5 Zonal depth ratio of lesions (Supplemental). This is a measurement of the depth of cartilage degeneration (e.g., including areas of

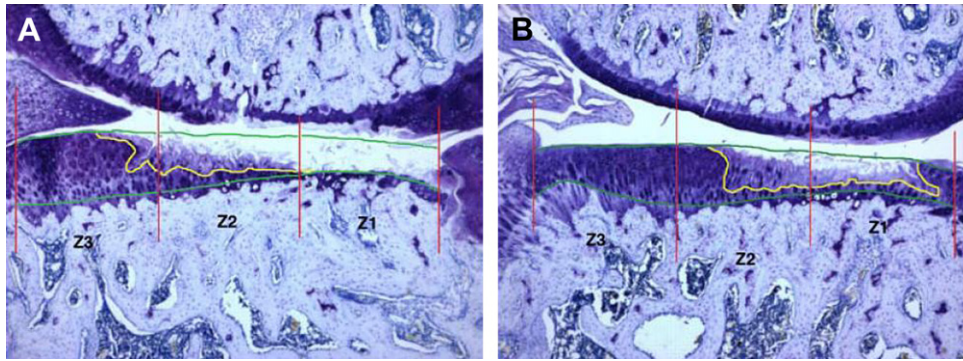


Fig. 4. #2 Cartilage degeneration score. Histological sections of the medial joint compartment of a rat with OA lesions following MMT. For evaluation, the tibial plateau is divided into three zones of equal width (marked by red vertical lines), with zone 1 (Z1) on the outside (medial edge of joint) and zone 3 (Z3) on the inside (adjacent to the central cruciate ligaments). The area of non-viable cartilage (significant chondrocyte loss but with collagen retention) is indicated by yellow tracing; the entire projected cartilage area is delineated by green tracing. **A.** Nearly all (99%) of the cartilage matrix has been lost or severely damaged in Z1 (grade of 5), 75% in Z2 (grade of 4), and 13% in Z3 (grade of 2). **B.** In this example of less severe general cartilage degeneration, 61% of the cartilage matrix has been lost or severely damaged in Z1 (grade of 4), 49% in Z2 (grade of 3), and there is no loss of cartilage matrix in Z3 (grade of 0).

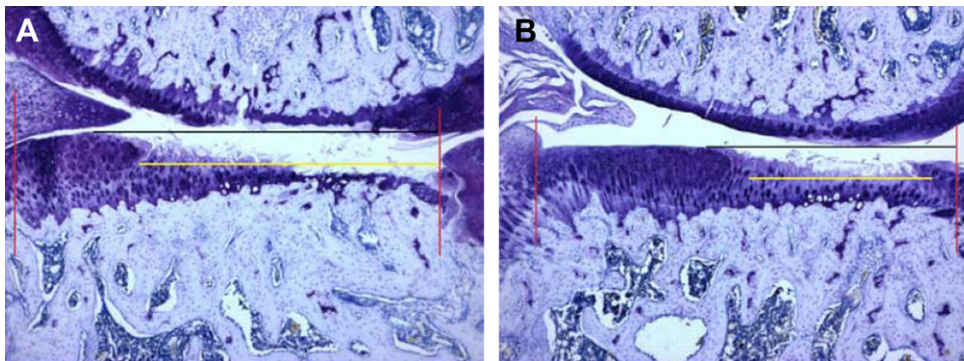


Fig. 5. #3 and #4 Total and significant cartilage degeneration width. #3. The total cartilage degeneration width (black horizontal line) represents the total extent of the tibial plateau affected by any type of degeneration (matrix fibrillation/loss, PG loss with or without chondrocyte death). The measurement is taken at the projected cartilage surface from the outer edge of the tibial plateau, adjacent to the osteophyte (outer red line), to the point at which the cartilage is normal (inner red line). #4. The significant cartilage degeneration width (yellow horizontal line) represents the width of tibial cartilage in which 50% or more of the original cartilage thickness is seriously compromised by collagen matrix loss or loss of 50% of chondrocytes (and concurrent PG) loss. **A.** Example of tibial plateau with large total and significant tibial cartilage degeneration width and **B.** example with smaller cartilage degeneration width.

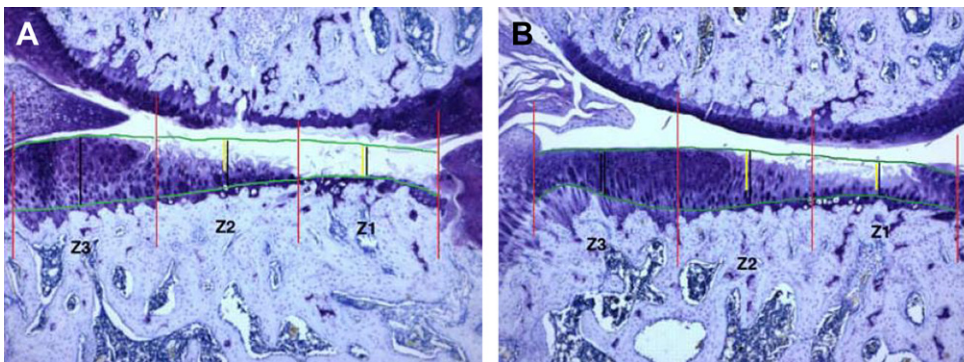


Fig. 6. #5 Zonal depth ratio of lesions. The lesion depth ratio is calculated by dividing the depth of the lesion (yellow line) by the thickness of the cartilage from projected articular surface to tidemark (black vertical line). These measurements are taken at the midpoint of each zone using an ocular micrometer. If care is taken to consistently measure the total depth (cartilage thickness) in the same location in each section, this parameter can also be used effectively with anabolic treatments to document cartilage thickening and increased matrix.

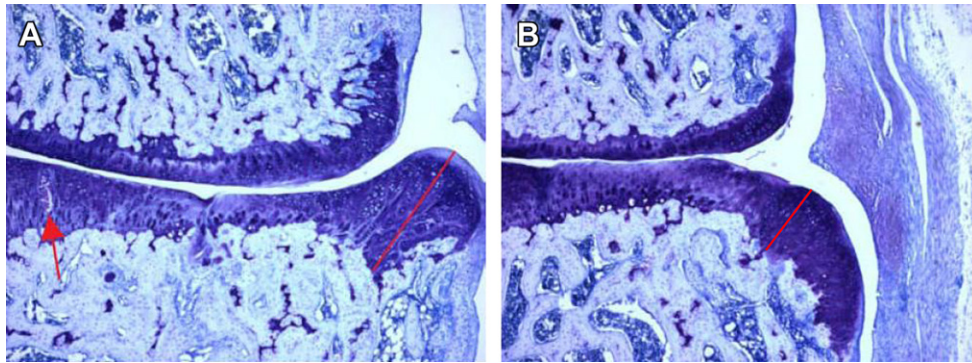


Fig. 7. #6 Osteophyte score. The largest osteophyte in the section (typically in the tibia) is measured from base to edge at the thickest point (red line) and then given a score based on that measurement. **A.** Large osteophyte. This section is from a SD rat after MMT, whereas all other sections shown here are from Lewis rats. Cartilage cysts (arrow) are common in aged SD rats and rarely seen in Lewis rats. **B.** Small osteophyte.

chondrocyte and PG loss, which may have good retention of collagenous matrix and no fibrillation) that is taken at the midpoint in each of the three zones across the tibial surface. The lesion depth ratio is calculated by dividing the micrometer depth of the area of degeneration by the thickness of the cartilage (both in micrometers), from projected cartilage surface to tidemark (Fig. 6).

#6 Osteophytes. The largest osteophyte in each section is measured (from the deepest point of its base at the chondro-osseous junction to the surface of the overlying cartilage at its thickest point) using an ocular micrometer (Fig. 7). Based on that measurement a grade is assigned according to Table III. The actual osteophyte measurement is also recorded.

#7 Calcified cartilage and subchondral bone damage score (Supplemental). This parameter is used to quantify effects of agents

on OA-associated changes in subchondral bone and calcified cartilage (Fig. 8; Table IV). The most severe lesion is scored in each section. It is usually located subjacent to the articular cartilage lesion of greatest severity.

#8 Synovial reaction (Supplemental). If the synovial membrane is abnormal, it is described and characterized with respect to inflammation type, extent, and severity. The score given in Table V characterizes surgery-induced inflammation based on increased numbers of synovial lining cell layers, proliferation of subsynovial tissue, and infiltration of inflammatory cells.

#9 Medial joint capsule repair. In addition, measurements may be made of the thickness of medial/collateral joint capsule repair in a non-tangential area of the section. (Fig. 9)

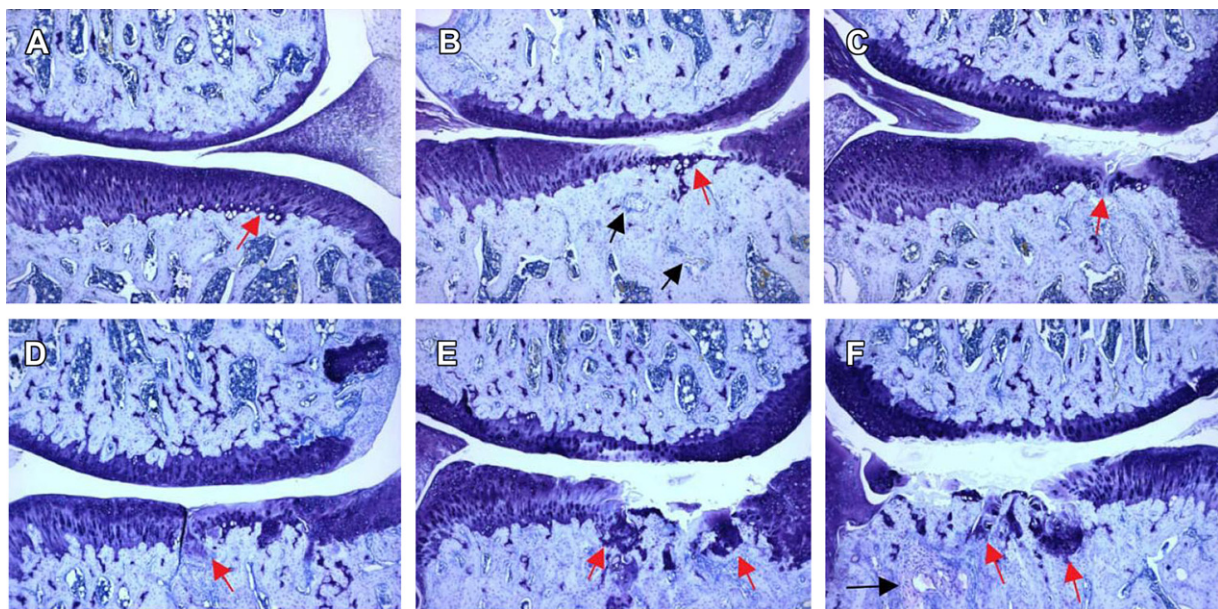


Fig. 8. #7 Calcified cartilage and subchondral bone damage. **A. Grade 0** – normal calcified cartilage and subchondral bone, however, slight increase in basophilia of the calcified cartilage in the central load-bearing area of the joint (red arrow). **B. Grade 1** – increased basophilia at the tidemark (red arrow) and minimal focal marrow changes (black arrows). Increased thickening of subchondral bone subjacent to the area of greatest cartilage lesion severity is observed in grade 1 and all higher grades. **C. Grade 2** – increased basophilia at the tidemark (red arrow), minimal to mild focal fragmentation of calcified cartilage of the tidemark, and mesenchymal change in marrow involving 1/4 of subchondral region under lesion. **D. Grade 3** – increased basophilia at the tidemark (red arrow), mild to marked multifocal fragmentation of calcified cartilage, and mesenchymal change in marrow of up to 3/4 of total area. Areas of marrow chondrogenesis are evident. **E. Grade 4** – increased basophilia at the tidemark (red arrows), marked to severe fragmentation of calcified cartilage, and marrow mesenchymal changes involving up to 3/4 of the area. Articular cartilage has collapsed into the epiphysis (see definite depression in surface cartilage). Basophilic areas under the area of collapse are a result of chondrogenesis in the bone marrow. **F. Grade 5** – marked to severe fragmentation of calcified cartilage and subchondral bone with collapse of cartilage and some chondrogenesis in the marrow (red arrows). Marrow mesenchymal changes involve up to 3/4 of the area and a large bone cyst (black arrow) is present. Articular cartilage has collapsed into the epiphysis to a depth of greater than 250 μ m from the tidemark with associated bone resorption.

Table III
#6 Osteophyte score

Parameter	Grade	Description
Osteophytes	0	Marginal zone proliferative changes <200 µm
	1	Small 200–299 µm
	2	Moderate 300–399 µm
	3	Large 400–499 µm
	4	Very large ≥500 µm

#10 Growth plate thickness (Supplemental). Growth plate thickness may be measured medially and laterally (two measures/joint), midway between the center of the physis and the medial (medial measurement) or lateral (lateral measurement) margin if an over-view of the sections suggests that differences in growth plate width are present. It is recommended to only measure growth plate thickness in sections of tibia, as these sections are more likely than those of the femur to be taken in a plane perpendicular to the growth plate in frontal sections.

Data analysis

If three sections per joint are analyzed, the mean ± standard error (SE) for each parameter or measurement is determined in order to obtain a total joint score. Statistical analysis is performed using ANOVA analysis. Measured parameters, such as cartilage

Table IV
#7 Calcified cartilage and subchondral bone damage score

Parameter	Grade	Description
Calcified cartilage and subchondral bone damage	0	No changes
	1	<ul style="list-style-type: none"> Increased basophilia at tidemark, no fragmentation of tidemark, no marrow changes or, if present, minimal and focal, increased thickening of subchondral bone subjacent to the area of greatest articular cartilage lesion severity.
	2	<ul style="list-style-type: none"> Increased basophilia at tidemark, minimal to mild focal fragmentation of calcified cartilage of tidemark, mesenchymal change in marrow (fibroblastic cells) involving about 1/4 of subchondral region under lesion, increased thickening of subchondral bone subjacent to the area of greatest articular cartilage lesion severity.
	3	<ul style="list-style-type: none"> Increased basophilia at tidemark, mild to marked fragmentation (multiple larger areas) of calcified cartilage/subchondral bone loss, mesenchymal change in marrow in up to 3/4 of total area, areas of marrow chondrogenesis may be evident but no major collapse of articular cartilage into epiphyseal bone (definite depression in surface).
	4	<ul style="list-style-type: none"> Increased basophilia at tidemark, marked to severe fragmentation of calcified cartilage, marrow mesenchymal change involves up to 3/4 of area, articular cartilage has collapsed into the epiphysis to a depth of 250 µm or less from tidemark (see definite depression in surface cartilage).
5	<ul style="list-style-type: none"> Increased basophilia at tidemark, marked to severe fragmentation of calcified cartilage, marrow mesenchymal change involves up to 3/4 of area, articular cartilage has collapsed into the epiphysis to a depth of greater than 250 µm from tidemark. 	

Table V
#8 Synovial membrane inflammation score

Parameter	Grade	Description
Synovial membrane inflammation	0	No changes (1–2 layers of synovial lining cells)
	1	Increased number of lining cell layers (≥3–4 layers) or <ul style="list-style-type: none"> slight proliferation of subsynovial tissue.
	2	<ul style="list-style-type: none"> Increased number of lining cell layers (≥3–4 layers) and/or proliferation of subsynovial tissue.
	3	<ul style="list-style-type: none"> Increased number of lining cell layers (>4 layers) and/or proliferation of subsynovial tissue and infiltration of few inflammatory cells.
	4	<ul style="list-style-type: none"> Increased number of lining cell layers (>4 layers) and/or proliferation of subsynovial tissue, infiltration of large number of inflammatory cells.

degeneration width, are analyzed using parametric ANOVA methods. When several treatment groups are compared, multiple comparison procedures such as Bonferroni or Tukey correction are used. Dunnett's test is applied when only comparisons to vehicle are of interest. Scored parameters are analyzed using a Kruskal–Wallis test with Dunn's post-test.

Reliability study

A set of photomicrographs of 18 rat knee joint histological sections was graded by 11 individuals using the recommended scoring scheme. The intra-class correlation coefficients (ICCs) depicting the inter-rater reliability of grading the features of the scoring system are shown in Table VI. The “expert” category encompasses graders who either had extensive experience with scoring OA lesions or received training with Alison Bendele. The “novice” category included all other graders. Results obtained by Alison Bendele (cartilage parameters) and Sonya Glasson (cartilage matrix loss widths), are considered to be the most accurate and were included in both groups in order to evaluate variability relative to the actual scores and measurements.

Correlation was very high in both the novice and expert groups, with the exception of two parameters. In the first case, which included cartilage degeneration scores in zone 3 of the medial tibia, ICC results were likely magnified due to the

Table VI
Reliability study. ICCs* depicting the inter-rater reliability within expert and novice groups for the grading of 18 histological sections each

Parameter	Histological feature	Experts (n = 4)	Novices (n = 8)
1	Cartilage matrix loss width – 0% Depth	0.94 (0.88, 0.97)	0.85 (0.74, 0.93)
	Cartilage matrix loss width – 100% Depth	0.99 (0.98, 1)	0.97 (0.94, 0.99)
	Cartilage matrix loss width – 50% Depth	0.95 (0.9, 0.98)	0.93 (0.87, 0.97)
2	3-Zone Tibial CDS† total	0.92 (0.85, 0.97)	0.88 (0.79, 0.94)
	Zone 1 Tibial CDS†	0.90 (0.81, 0.96)	0.86 (0.76, 0.94)
	Zone 2 Tibial CDS†	0.92 (0.85, 0.97)	0.90 (0.82, 0.95)
	Zone 3 Tibial CDS†	0.67 (0.46, 0.84)	0.44 (0.26, 0.66)
	Femoral CDS†	0.92 (0.85, 0.97)	0.88 (0.79, 0.94)
3	Total tibial cartilage degeneration width	0.62 (0.4, 0.81)	0.50 (0.32, 0.71)
4	Significant tibial cartilage degeneration width	0.89 (0.79, 0.95)	0.77 (0.63, 0.89)
5	Osteophyte measurement	0.95 (0.9, 0.98)	0.97 (0.94, 0.99)
	Osteophyte score	0.91 (0.82, 0.96)	0.95 (0.91, 0.98)
	Total joint score w/o femur	0.93 (0.86, 0.97)	0.92 (0.86, 0.96)
	Total joint score	0.93 (0.86, 0.97)	0.92 (0.86, 0.96)

* 95% Confidence intervals for each ICC are listed in parenthesis.

† CDS = cartilage degeneration score.

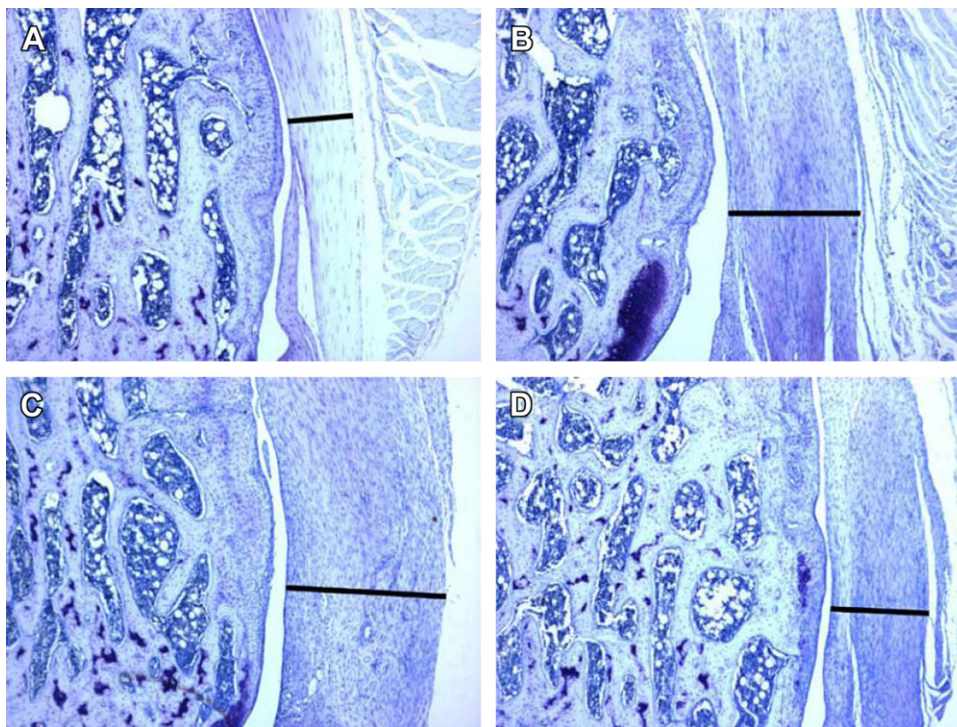


Fig. 9. #9 Medial joint capsule repair. A. Normal medial joint capsule (no surgery). B. Medial joint capsule from a vehicle-treated animal 3 weeks after MMT surgery. C. Medial joint capsule from an animal treated with compound that enhanced repair 3 weeks after MMT surgery. D. Medial joint capsule from an animal treated with compound that inhibited repair 3 weeks after MMT surgery. Thickness of the medial joint capsule is measured as indicated by the black bar.

extremely low scores and lack of variation typically seen in this region. The other parameter with low correlation, which was total tibial cartilage degeneration width, involves more subtle changes in the cartilage, which may not have been as evident in the photomicrographs as they would be when viewed directly in the microscope.

Discussion

This work is the result of the efforts of an experienced group of rat OA investigators to develop and describe a reproducible and accurate scheme for the histological evaluation of lesions of OA in this species. The validation study revealed that this scheme, while not as simple to use as some other modified Mankin scores, may be used reproducibly by individuals with variable experience in the histopathologic evaluation of OA. In addition, this scheme has been used effectively in multiple studies for efficacy evaluation of disease-modifying OA treatments in experimentally-induced OA in rats^{5,23,29}.

Disclosures

Sub-coordinator Nicole Gerwin is an employee of and holds stock in Novartis.

Sub-coordinator Alison Bendele is Director of BolderBioPATH Inc., a contract research laboratory for preclinical studies in arthritis.

Committee member Sonya Glasson is an employee of and holds stock in Pfizer.

Committee member Cathy S. Carlson is employed at the College of Veterinary Medicine, University of Minnesota.

Conflict of interest

No author has any conflict of interest related to this work.

Acknowledgements

We thank Ben Kriederman (Histotox), Brian Omura (Bolder-BioPATH), Connie Kilwinski (Centocor), Julio Tejada (Pfizer), Margaret McNulty (Carlson laboratory), Nicole Schmitz (Aigner laboratory), Phil Bendele (BolderBioPATH), and Steve Settle (Pfizer) for participating in the reliability study. No external sources of funding were provided for this work except that the printing costs were supported by an unrestricted educational grant to OARSI by Bayer, Expanscience, Genzyme, Lilly, MerckSerono, Novartis, Pfizer, SanofiAventis, and Servier. The work performed was not influenced at any stage by the support provided.

Supplementary data

Supplementary data associated with this article can be found in the online version at doi:10.1016/j.joca.2010.05.030.

References

1. Gyarmati J, Foldes I, Kern M, Kiss I. Morphological studies on the articular cartilage of old rats. *Acta Morphol Hung* 1987;35 (3–4):111–24.
2. Smale G, Bendele A, Horton WRJ. Comparison of age-associated degeneration of articular cartilage in Wistar and Fischer 344 rats. *Lab Anim Sci* 1995;45(2):191–4.
3. Bendele AM. Animal models of osteoarthritis. *J Musculoskelet Neuronal Interact* 2001;1(4):363–76.
4. Janusz MJ, Bendele AM, Brown KK, Taiwo YO, Hsieh L, Heitmeyer SA. Induction of osteoarthritis in the rat by surgical tear of the meniscus: inhibition of joint damage by a matrix metalloproteinase inhibitor. *Osteoarthritis and Cartilage* 2002;10(10):785–91.

5. Moore EE, Bendele AM, Thompson DL, Littau A, Waggle KS, Reardon B, et al. Fibroblast growth factor-18 stimulates chondrogenesis and cartilage repair in a rat model of injury-induced osteoarthritis. *Osteoarthritis and Cartilage* 2005;13(7):623–31.
6. Williams JM, Felten DL, Peterson RG, O'Connor BL. Effects of surgically induced instability on rat knee articular cartilage. *J Anat* 1982;134(Pt 1):103–9.
7. Stoop R, Buma P, van der Kraan PM, Hollander AP, Billingham RC, Poole AR, et al. Differences in type II collagen degradation between peripheral and central cartilage of rat stifle joints after cranial cruciate ligament transection. *Arthritis Rheum* 2000;43(9):2121–31.
8. Karahan S, Kincaid SA, Kammermann JR, Wright JC. Evaluation of the rat stifle joint after transection of the cranial cruciate ligament and partial medial meniscectomy. *Comp Med* 2001;51(6):504–12.
9. Hayami T, Pickarski M, Zhuo Y, Wesolowski GA, Rodan GA, Duong LT. Characterization of articular cartilage and subchondral bone changes in the rat anterior cruciate ligament transection and meniscectomized models of osteoarthritis. *Bone* 2006;38(2):234–43.
10. Appleton CT, McErlain DD, Pitelka V, Schwartz N, Bernier SM, Henry JL, et al. Forced mobilization accelerates pathogenesis: characterization of a pre-clinical surgical model of osteoarthritis. *Arthritis Res Ther* 2007;9(1):R13.
11. Lozoya KA, Flores JB. A novel rat osteoarthrosis model to assess apoptosis and matrix degradation. *Pathol Res Pract* 2000;196(11):729–45.
12. Galois L, Etienne S, Grossin L, Watrin-Pinzano A, Cournil-Henrionnet C, Loeuille D, et al. Dose-response relationship for exercise on severity of experimental osteoarthritis in rats: a pilot study. *Osteoarthritis and Cartilage* 2004;12(10):779–86.
13. Kalbhen DA. Chemical model of osteoarthritis—a pharmacological evaluation. *J Rheumatol* 1987;14(Suppl 14):130–131.
14. Guingamp C, Gegout-Pottie P, Philippe L, Terlain B, Netter P, Gillet P. Mono-iodoacetate-induced experimental osteoarthritis: a dose-response study of loss of mobility, morphology, and biochemistry. *Arthritis Rheum* 1997;40(9):1670–9.
15. Guzman RE, Evans MG, Bove S, Morenko B, Kilgore K. Mono-iodoacetate-induced histologic changes in subchondral bone and articular cartilage of rat femorotibial joints: an animal model of osteoarthritis. *Toxicol Pathol* 2003;31(6):619–24.
16. Janusz MJ, Little CB, King LE, Hookfin EB, Brown KK, Heitmeyer SA, et al. Detection of aggrecanase- and MMP-generated catabolic neopeptides in the rat iodoacetate model of cartilage degeneration. *Osteoarthritis and Cartilage* 2004;12(9):720–8.
17. Gelse K, von der Mark K, Aigner T, Park J, Schneider H. Articular cartilage repair by gene therapy using growth factor-producing mesenchymal cells. *Arthritis Rheum* 2003;48(2):430–41.
18. Ikeda T, Kubo T, Nakanishi T, Arai Y, Kobayashi K, Mazda O, et al. Ex vivo gene delivery using an adenovirus vector in treatment for cartilage defects. *J Rheumatol* 2000;27(4):990–6.
19. Kuroda R, Usas A, Kubo S, Corsi K, Peng H, Rose T, et al. Cartilage repair using bone morphogenetic protein 4 and muscle-derived stem cells. *Arthritis Rheum* 2006;54(2):433–42.
20. Nishida T, Kubota S, Kojima S, Kuboki T, Nakao K, Kushibiki T, et al. Regeneration of defects in articular cartilage in rat knee joints by CCN2 (Connective Tissue Growth Factor). *J Bone Miner Res* 2004;19(8):1308–19.
21. Hoegh-Andersen P, Tanko L, Andersen T, Lundberg C, Mo J, Heegaard AM, et al. Ovariectomized rats as a model of postmenopausal osteoarthritis: validation and application. *Arthritis Res Ther* 2004;6(2):R169–80.
22. Ekenstedt KJ, Sonntag WE, Loeser RF, Lindgren BR, Carlson CS. Effects of chronic growth hormone and insulin-like growth factor 1 deficiency on osteoarthritis severity in rat knee joints. *Arthritis Rheum* 2006;54(12):3850–8.
23. Baragi VM, Becher G, Bendele AM, Biesinger R, Bluhm H, Boer J, et al. A new class of potent matrix metalloproteinase 13 inhibitors for potential treatment of osteoarthritis: evidence of histologic and clinical efficacy without musculoskeletal toxicity in rat models. *Arthritis Rheum* 2009;60(7):2008–18.
24. Fernihough J, Gentry C, Malcangio M, Fox A, Rediske J, Pellas T, et al. Pain related behaviour in two models of osteoarthritis in the rat knee. *Pain* 2004;112(1–2):83–93.
25. Bove SE, Laemont KD, Brooker RM, Osborn MN, Sanchez BM, Guzman RE, et al. Surgically induced osteoarthritis in the rat results in the development of both osteoarthritis-like joint pain and secondary hyperalgesia. *Osteoarthritis and Cartilage* 2006;14(10):1041–8.
26. Hayami T, Pickarski M, Wesolowski GA, McLane J, Bone A, Destefano J, et al. The role of subchondral bone remodeling in osteoarthritis: reduction of cartilage degeneration and prevention of osteophyte formation by alendronate in the rat anterior cruciate ligament transection model. *Arthritis Rheum* 2004;50(4):1193–206.
27. Hyllested JL, Veje K, Ostergaard K. Histochemical studies of the extracellular matrix of human articular cartilage—a review. *Osteoarthritis and Cartilage* 2002;10(5):333–43.
28. Mankin HJ, Dorfman HA, Lippiello L, Zarins A. Biochemical and metabolic abnormalities in articular cartilage from osteoarthritic human hips: II. Correlation of morphology with biochemical and metabolic data. *J Bone Joint Surg Am* 1971;53(3):523–37.
29. Flannery C, Zollner R, Corcoran C, Jones A, Root A, Rivera-Bermúdez M, et al. Prevention of cartilage degeneration in a rat model of osteoarthritis by intraarticular treatment with recombinant lubricin. *Arthritis Rheum* 2009;60(3):840–7.
30. Yorimitsu M, Nishida K, Shimizu A, Doi H, Miyazawa S, Komiyama T, et al. Intra-articular injection of interleukin-4 decreases nitric oxide production by chondrocytes and ameliorates subsequent destruction of cartilage in instability-induced osteoarthritis in rat knee joints. *Osteoarthritis and Cartilage* 2008;16(7):764–71.
31. Pritzker KPH, Gay S, Jimenez SA, Ostergaard K, Pelletier JP, Revell PA, et al. Osteoarthritis cartilage histopathology: grading and staging. *Osteoarthritis and Cartilage* 2006;14(1):13–29.
32. Wancket LM, Baragi V, Bove S, Kilgore K, Korytko PJ, Guzman RE. Anatomical localization of cartilage degradation markers in a surgically induced rat osteoarthritis Model. *Toxicol Pathol* 2005;33(4):484–9.
33. Glasson S, Bendele AM, Sum P-E, Tam S, Tajeda J, Rivera-Bermúdez M, et al. Selective aggrecanase inhibition is disease modifying and pain alleviating in a rat meniscal tear model of osteoarthritis. *Osteoarthritis and Cartilage* 2009;17(Suppl.1):S56. Ref Type: Abstract.
34. Jean YH, Wen ZH, Chang YC, Hsieh SP, Tang CC, Wang YH, et al. Intra-articular injection of the cyclooxygenase-2 inhibitor parecoxib attenuates osteoarthritis progression in anterior cruciate ligament-transected knee in rats: role of excitatory amino acids. *Osteoarthritis and Cartilage* 2007;15(6):638–45.
35. Lin YS, Huang MH, Chai CY. Effects of helium-neon laser on the mucopolysaccharide induction in experimental osteoarthritic cartilage. *Osteoarthritis and Cartilage* 2006;14(4):377–83.
36. Yeh T, Wen Z, Lee H, Lee C, Yang Z, Jean Y, et al. Intra-articular injection of collagenase induced experimental osteoarthritis of the lumbar facet joint in rats. *Eur Spine J* 2008;17(5):734–42.
37. Salo PT, Hogervorst T, Seerattan R, Rucker D, Bray RC. Selective joint denervation promotes knee osteoarthritis in the aging rat. *J Ortho Res* 2002;20(6):1256–64.